Master's thesis

NTNU
Norwegian University of Science and Technology
Faculty of Medicine and Health Sciences
Department of Clinical and Molecular Medicine

Md Abu Jafar Sujan

Lipocalin 2 is expressed in MLO-Y4 osteocytes and regulated by the peroxisome proliferator activated receptor agonist fenofibrate

Master's thesis in Molecular Medicine

Supervisor: Unni Syversen

June 2020

NTNU
Norwegian University of
Science and Technology

Md Abu Jafar Sujan

Lipocalin 2 is expressed in MLO-Y4 osteocytes and regulated by the peroxisome proliferator activated receptor α agonist fenofibrate

Master of Science in Molecular Medicine

Principal supervisor: Unni Syversen

Co-supervisors: Ingrid K. Hals, Astrid Kamilla Stunes

June 2020

Norwegian University of Science and Technology

Faculty of Medicine and Health Sciences

Department of Clinical and Molecular Medicine

NTNU

Norwegian University of Science and Technology

Abstract

Background: Lipocalin 2 is highly expressed and secreted from osteoblasts in mice. Lately, bone-derived lipocalin 2 has been shown to suppress appetite by binding to the MC4R in hypothalamus. In the present study we wanted to examine whether the PPARα agonist fenofibrate exerts its weight-reducing effect through stimulation of lipocalin 2 secretion.

Methods: The murine pre-osteoblast and osteocyte cell lines (MC3T3-E1 and MLO-Y4) were incubated with DMSO (control) and fenofibrate dissolved in DMSO for 24 and 72 hours. MC3T3-E1 cells were exposed to fenofibrate 10 µM, and MLO-Y4 cells to 1 and 10 µM. Lipocalin 2 in cell medium and lysate was measured by ELISA, and lipocalin 2 mRNA in MLO-Y4 cells by RTPCR. Lipocalin 2 was also analyzed in plasma from ovariectomized (OVX) rats exposed to fenofibrate (90 mg/kg/d) for eight weeks and in OVX controls.

Results: Lipocalin 2 mRNA was significantly and highly expressed in MLO-Y4 cells after exposure to fenofibrate 1 and 10 µM for 24 hours. No significant differences in lipocalin levels were observed in cell medium or lysate from MC3T3-E1 and MLO-Y4 cells after incubation with fenofibrate. The highest levels of lipocalin 2 were seen after exposure of MLO-Y4 cells to fenofibrate 1 µM for 72 hours. The amount of lipocalin 2 appeared to be modest in MC3T3-E1 cells. Plasma levels of lipocalin 2 were higher in OVX rats exposed to fenofibrate than in controls, however, not significantly.

Conclusion: We show for the first time that lipocalin 2 is expressed, translated and secreted from the osteocyte cell line MLO-Y4, and that lipocalin 2 mRNA expression is upregulated by fenofibrate.

Acknowledgements

I would first like to thank my thesis supervisor Prof. Unni Syversen of the Department of Clinical and Molecular Medicine at Norwegian University of Science and Technology. The door to her office was always open whenever I ran into a trouble spot or had a question about my research or writing. She consistently allowed this paper to be my own work but steered me in the right the direction whenever she thought I needed it.

I would also like to thank my co-supervisor Dr. Ingrid K. Hals for her numerous theoretical and practical guidance that lead me to accomplish my thesis precisely. In addition, a thank you to my other co-supervisor Dr. Astrid Kamilla Stunes for the constant support in the lab work before and during the COVID-19 pandemic and for arranging the journal club to discuss academic papers and lab progresses. I am thankful to Mr. Zekarias Zinbot for helping with the project during the COVID-19 pandemic. Without their passionate participation and input, the research could not have been successfully conducted.

I would like to thank Mathilde Homstad and Vincent Jongen, my fellow members in the bone and endocrinology group for their help and collaboration during my research.

Finally, I must express my very profound gratitude to my parents for providing me with unfailing support and continuous encouragement throughout my years of study and through the process of researching and writing this thesis. This accomplishment would not have been possible without them. Thank you.

Table of contents

List of figures

List of tables

Abbreviations

1,25(OH)2D3	1,25-dihydroxyvitamin D3
ATCC	American Type Culture Collection
BALP	Bone-specific alkaline phosphatase
BMD	Bone mineral density
C/EBP	CCAAT enhancer binding protein
cAMP	Cyclic AMP
cDNA	Complementary DNA
CTR	Control
DM	Diabetes melitus[1]
DMSO	Dimethyl sulfoxide
dsDNA	Double stranded DNA
ECM	Extracellular matrix
EDTA	Ethylenediaminetetraacetic acid
ELISA	Enzyme-linked immunosorbent assay
EPA	Eicosapentanoic acid
FA	Fatty acid
FCS	Fetal calf serum
FGF 23	Fibroblast growth factor 23
GAPDH	Glyceraldehyde-3-phosphate dehydrogenase
GlaOCN	Carboxylated OCN
GluOCN	Undercarboxylated OCN
GLUT	Glucose transporter
GPCR	G protein-coupled receptor
GPRC6A	G-protein-coupled receptor class C group 6 member A
HDL	High density lipoprotein
HFD	High-fat diet
HRP	Horseradish peroxidase
HSC	Hematopoietic stem cell
IFNγ	Interferon γ
IL-17	Interleukin 17
IL-1β	Interleukin 1β
IL-6	Interleukin 6
ING1b	Inhibitors of Growth 1b

JAK	Janus kinase
LPS	Lipopolysaccharide
LRP	Lipoprotein receptor-related proteins
MC4R	Melanocortin 4 receptor
MEM-α	Minimal Essential Medium-α
MMP	Matrix metalloproteinase
MSC	Mesenchymal stem cell
MUFA	Monounsaturated fatty acids
NFAT1	Nuclear factor of activated T-cells 1
NF-κB	Nuclear factor-κB
NGAL	Neutrophil gelatinase associated lipocalin
OCN	Osteocalcin
OPG	Osteoprotegerin
OVX	Ovariectomized
PBS	Phosphate buffered saline
PCR	Polymerase chain reaction
PPAR	Peroxisome proliferator activated receptor
PPRE	PPAR response element
PUFA	Polyunsaturated fatty acid
PTH	Parathyroid hormone
PVN	Paraventricular nucleus
RANK	Receptor activator of the NF-κB
RANKL	Receptor activator of NF-κB ligand
RNA	Ribonucleic acid
RTPCR	Real time polymerase chain reaction
SEM	Standard error of mean
STAT	Signal transducer and activator of transcription
TNFα	Tumor necrosis factor α
TZD	Thiazolidinedione
WT	Wild type
αMSH	α melanocyte stimulating hormone

1. Introduction

1.1. Bone

The skeleton accounts for approximately 15% of total body weight and is one of the largest organ systems in the human body. It provides mechanical support for stature and locomotion in addition to providing protection for vital organs. Besides these functions, bone also acts as an important reservoir for several minerals including calcium, phosphate, magnesium and sodium.[2,3]

Bone is a mineralized connective tissue that exhibits four types of cells: osteoblasts, bone lining cells, osteocytes, and osteoclasts.[4] Osteoblasts differentiate from mesenchymal stem cells (MSCs) and comprise 5% of all bone cells. They are responsible for the synthesis of type I collagen and several non-collagenous proteins, as well as deposition of mineralized matrix to facilitate the formation of bone.[5,6] Osteoblasts differentiate to osteocytes which are embedded in the bone matrix and constitute 90% of total bone cells.[7] The osteocytes translate mechanical strain into biochemical signals and are the key cells in regulation of bone metabolism.[8]

Osteoclasts differentiate from hematopoietic stem cells (HSCs).[9] They synthesize vacuolar-ATPases which are transported to the ruffled border membrane on the bone surface, where they pump protons into resorption lacunae to dissolve hydroxyapatite. The resulting low pH in the resorption lacunae achieved by the large number of proton pumps activates matrix metalloproteinases (MMPs) and cysteine proteinases to degrade the collagenous bone matrix.[10] Thereafter, signal substances are released from the bone matrix and from the osteoclast to initiate bone formation by the osteoblasts. The function of bone lining cells is not settled, but they seem to be involved in the coupling between bone resorption and formation.[5] The blood vessels in the bone also play a role in bone formation and provide a niche for HSCs that reside in the bone marrow.[11,12]

1.2. Bone homeostasis

Bone undergoes constant remodeling of its microarchitecture and composition throughout an individual's lifetime to facilitate its classical functions and to maintain the integrity of the skeleton. Bone remodeling goes through two processes, removal of old or damaged bone by osteoclasts followed by replacement with new bone by osteoblasts.[7,13] Osteoblasts, osteocytes, and osteoclasts interact with each other and maintain the remodeling and architecture of skeleton by synthesizing and secreting paracrine signaling molecules, including growth factors, cytokines and chemokines.

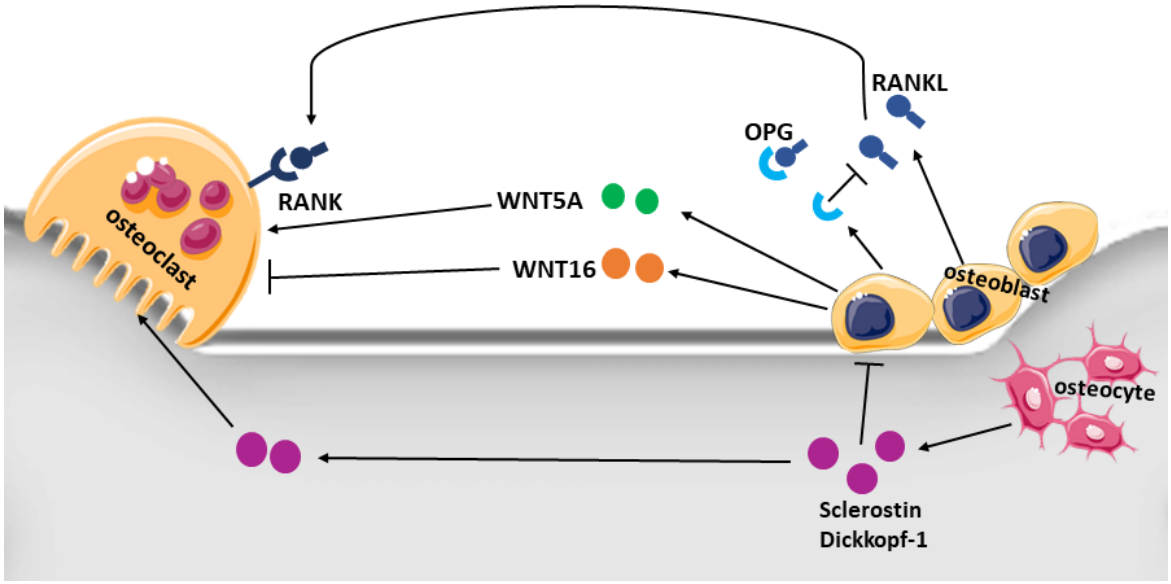

Figure 1.1: Paracrine signaling by bone cells.

Osteoblast expression of RANKL promotes osteoclast activity, whereas OPG inhibits osteoclastogenesis. Osteocyte secretion of sclerostin and Dickkopf-1 inhibits osteoblasts through blocking Wnt signaling. The figure was modified from "Paracrine and endocrine actions of bone" by Y Han et al.[1]

Osteoblasts and osteocytes regulate osteoclastogenesis and bone resorption by secreting receptor activator of NF-κB ligand (RANKL)[14-16], anti-osteoclastogenic factors such as osteoprotegerin (OPG)[17-19]. RANKL is necessary for the formation, fusion, activation, and survival of osteoclasts by binding to its receptor, receptor activator of the NF-κB (RANK), on osteoclasts and its precursors.[20] OPG acts as a soluble decoy receptor of RANKL to antagonize the effects of RANKL and interrupt the crosstalk between osteoblasts and osteoclasts.[21]The Wnt/β-catenin signaling pathway is the main regulator of bone formation. This pathway is important in osteoblasts for proliferation, differentiation and synthesis of bone matrix[22], whereas osteocytes use the Wnt/β-catenin pathway to transmit signals of mechanical loading to cells on the bone surface. Osteocytes secret sclerostin, a negative regulator of the Wnt/βcatenin signaling pathway by binding to the Wnt co-receptors, low-density lipoprotein receptor-related proteins 5 and 6 (LRP5 and LRP6). Sclerostin inhibits osteoblast differentiation and subsequently bone formation in a paracrine manner[23]. The pathway is triggered by crosstalk with the prostaglandin pathway in response to loading, resulting in a decrease in negative regulators of bone formation such as sclerostin and Dickkopf-1.[24] Bone-specific alkaline phosphatase (BALP) is secreted by osteoblasts in response to vitamin D.

BALP promotes bone mineralization by reducing the level of pyrophosphate which is a naturally occurring inhibitor of mineralization.[25]

1.3. Bone – an endocrine organ

1.3.1. Fibroblast growth factor 23

The skeleton has recently been recognized as an endocrine organ. Genetic analyses of human familial disorders of phosphate homeostasis led to the discovery of bone-derived fibroblast growth factor 23 (FGF23)[26]. Subsequent studies have revealed that it is principally secreted by osteocytes.[27] FGF23 plays important roles in modulating phosphate homeostasis. It suppresses the expression of sodium-phosphate cotransporters in the proximal tubules of the kidney, thereby inhibiting phosphate reabsorption.[28] The production of 1,25-dihydroxyvitamin D3 [1,25(OH)2D3] is also suppressed through inhibition of 1α-hydroxylase, resulting in attenuation of intestinal phosphate absorption. Consequently, FGF23 reduces the circulating phosphate levels[29,30].

1.3.2. Osteocalcin

Osteocalcin (OCN) is a bone-derived hormone that is proposed to regulate the biological processes of multiple organs including bone, adipose, liver, muscle, pancreas, testes, and brain[2,6,31-38]. It is the most abundant osteoblast-specific non-collagenous protein. Insulin signaling in osteoblasts leads to reduced OPG expression and increased osteoclast activity.[39] Osteoclasts are responsible for increasing the circulating level of bioactive undercarboxylated OCN (GluOCN).[40]

OCN-null mice exhibit abnormal quantities of body fat and reduced peripheral insulin sensitivity, impaired glucose metabolism, liver steatosis and inflammation in white adipose tissue.[34,39,41] Co-culture assays show that OCN secreted by osteoblasts promote β-cell proliferation, insulin secretion and sensitivity, indicating that OCN may play a role in the regulation of energy metabolism.[35] OCN regulates the uptake and catabolism of glucose and fatty acids (FAs) in muscle during exercise.[42] Moreover, OCN and IL-6 mediate the crosstalk between bone and skeletal muscle by modulating adaptation to exercise.[33] OCN has also been shown to stimulate testosterone synthesis.[43]. Finally, a role of OCN in the fight or flight response has been revealed.[44]

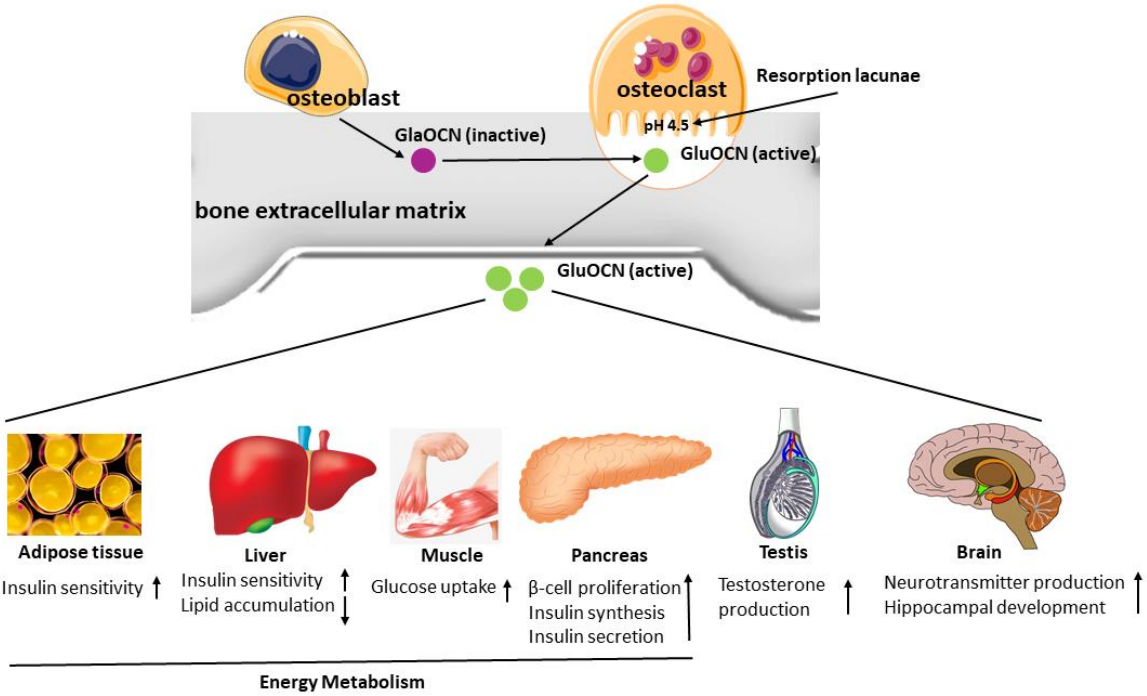

Figure 1.2: Endocrine functions of OCN.

OCN is C-carboxylated (GlaOCN) and secreted by osteoblasts into bone extracellular matrix (ECM). The acidic pH (~4.5) in the resorption lacunae formed by osteoclasts decarboxylates GlaOCN into undercarboxylated active osteocalcin (GluOCN), which enters the circulation to act as a hormone. GluOCN regulates energy metabolism via enhancement of glucose uptake in muscle, insulin production in the pancreas, insulin sensitivity in the liver and adipose tissue and promotion of β-cell proliferation in the pancreas. In addition, OCN stimulates testosterone synthesis in Leydig cells. It also improves cognitive function of the brain through an increase in neurotransmitter synthesis and facilitation of hippocampus development. The figure was modified from "Paracrine and endocrine actions of bone" by Y Han et al.[1]

Whether the findings in rodents also apply to humans is not settled. In a cross-sectional analysis, osteocalcin was inversely associated with fasting plasma glucose, fasting insulin, a parameter of insulin resistance [homeostasis model assessment for insulin resistance (HOMA-IR)], and fat mass.[45]

1.3.3. Lipocalin 2

Lipocalin 2 adds to the list of hormones derived from bone cells. It is also known as neutrophil gelatinase associated lipocalin (NGAL) which is the term applied in humans.[46] Lipocalin 2 is a 25-kDa glycoprotein that binds and transports small hydrophobic molecules, such as retinoic acid, hormones, and fatty acids.[47] It was initially discovered as a matrix metalloproteinase 9 (MMP-9) binding protein that attenuated MMP-9 degradation.[48] Lipocalin 2 has been proposed

to exert many different functions in humans, including a role in iron homeostasis, infection and inflammation.[49]

Lipocalin 2 is produced and secreted by adipocytes and has therefore been classified as an adipokine.[50] It is also expressed in many other tissues, including uterus, bone marrow, immune system, and malignant tumors.[48,51-54] Lipocalin 2 expression was detected in murine osteoblasts[55], and a 10-fold higher expression was observed in bone than in fat or any other tissue.[56]

The expression of the lipocalin 2 gene is stimulated by lipopolysaccharide (LPS) and cytokines including as tumor necrosis factor α (TNFα), interleukin 1β (IL-1β), interleukin 6 (IL-6), interleukin 17 (IL-17) and interferon γ (IFNγ).[50,57,58] Factors such as fasting and cold stress, fatty acids (palmitate and oleate), H2O2 and dexamethasone also stimulate expression of lipocalin 2 gene.[50,59-61] Lipocalin 2 expression and secretion by insulin is dose-dependent; this insulin effect is significantly abolished in the presence of low concentration of glucose.[50]

The inducing factors initiate a cascade of intracellular pathways such as the nuclear factor-κB (NF-κB) pathway, Janus kinase (JAK)-signal transducer and activator of transcription (STAT) pathway and activate nuclear factors that lead to expression of lipocalin 2.[50] IFNγ and TNFα have been reported to induce lipocalin 2 expression in both murine and human adipocytes.[62] The promoter region of lipocalin 2 contains the binding sites for NF-κB, STAT1, nuclear factor of activated T-cells 1 (NFAT1) and CCAAT enhancer binding protein (C/EBP) as well as several nuclear receptor response elements including glucocorticoid response element, retinoic acid receptor response element, and estrogen response element.[57,60,63] The intracellular pathways and the binding sites in the promoter region of lipocalin 2 suggest that lipocalin 2 is involved in among others inflammation, bone metabolism, energy metabolism and appetite control.

1.3.3.1. Lipocalin 2, bone and energy metabolism

Adipocytes were initially regarded as the main lipocalin 2-producing cells.[50] This was challenged by Mosialou et al., who showed that lipocalin 2 level in WT osteoblasts was 10-fold higher than in adipocytes.[56] Capulli et al. showed that lipocalin 2–/– mice exhibited a marked osteopenic phenotype due to reduced osteoblast number and activity, with no changes in osteoclast parameters.[64] The authors suggested that the impairment of GLUT1 expression in lipocalin 2–/– bone could contribute to the low bone formation.[64] Lipocalin 2 overexpression reduces osteoblast differentiation and stimulates the production of interleukin 6 (IL-6) and

receptor activator of NF-kB ligand (RANKL), which in turn promotes osteoclastogenesis.[65] These data support that lipocalin 2 plays a role in bone homeostasis.

Mosialou et al. showed that bone-derived lipocalin 2 suppresses appetite.[56] They observed that circulating lipocalin 2 crosses the blood–brain barrier and accumulates mainly in the hypothalamus where it activates neurons in the paraventricular nucleus (PVN). The PVN is involved in feeding regulation partly as the result of actions of the well-established melanocortin 4 receptor (MC4R) anorexigenic pathway. Lipocalin 2 binds to MC4R with an affinity similar to that of its ligand, α melanocyte–stimulating hormone (αMSH) resulting in reduction of food intake, increase in energy expenditure and a subsequent loss of body weight.[56] The ability of lipocalin 2 to suppress appetite is blunted in MC4R-depleted mice, resulting in hyperphagia and early-onset obesity, increased fat mass, decreased energy expenditure, and hyperinsulinemia.[56] Thus, MC4R seems to play the central role in mediating the anorexigenic response of lipocalin 2.

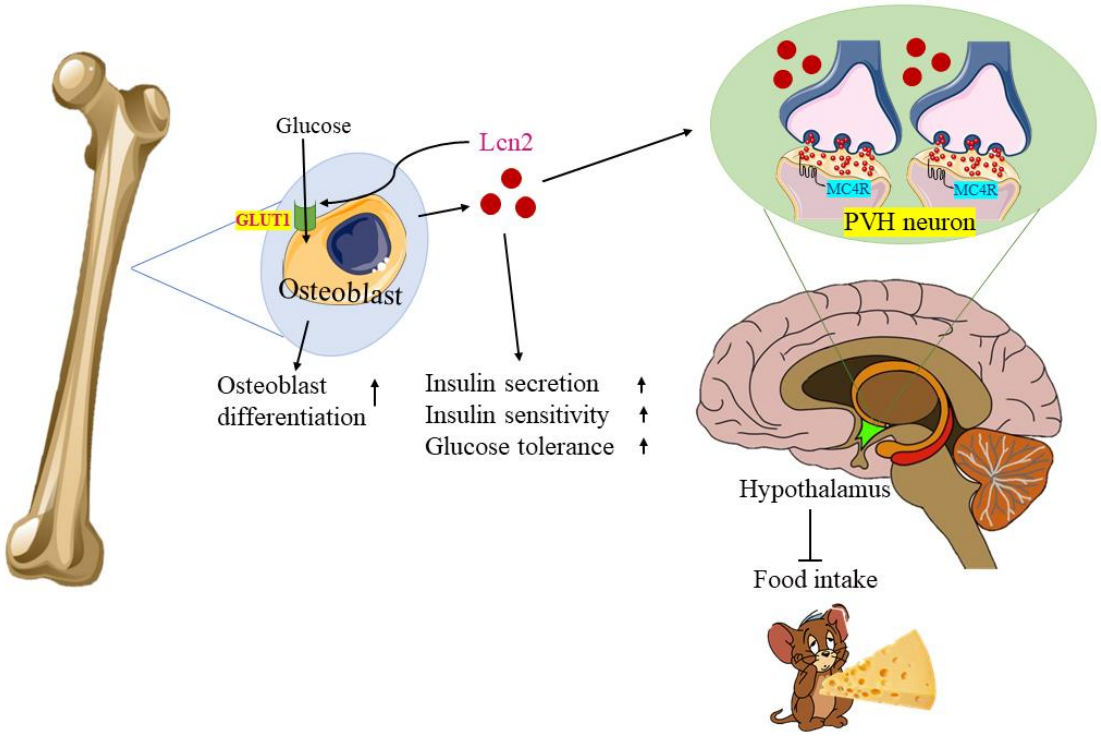

Figure 1.3: Effect of lipocalin 2 on appetite control and metabolism.

Osteoblast expression of lipocalin 2 lowers appetite by binding to MC4R in PVN of hypothalamus, thereby reducing food intake. It increases insulin secretion, sensitivity and glucose tolerance. Lipocalin 2 stimulates osteoblast differentiation by inducing glucose uptake through GLUT1 channels. The figure was modified from "Paracrine and endocrine actions of bone" by Y Han et al.[1]

The lipocalin 2/MC4R interaction has also been observed in humans as some obese people carrying mutations in MC4R had elevated lipocalin 2 plasma levels as compared with weight-matched people without mutations. The authors proposed that lipocalin 2 level is increased in the case of desensitization or inactivation of its associated receptor to overcome resistance and reestablish homeostasis.[56]

Paton et al. showed that circulating lipocalin 2 levels increased threefold 1 to 3 hours postprandially in mice.[66] Additionally, they observed elevated levels of lipocalin 2 were found in normal-weight women following a high-fat meal, whereas this regulation was lost in obese women. Chronic administration of exogenous lipocalin 2 to lean and obese mice decreases food intake, fat mass, and body weight gain, and improves glucose homeostasis and energy expenditure.[56,66] In a recent study, the mRNA expression of lipocalin 2 was upregulated in white and brown adipose tissues as well as liver during fasting and cold stress in mice.[50] Hence, taken together, these studies provide evidence for a physiological role of lipocalin 2 in the regulation of appetite and energy metabolism.

1.4. Peroxisome proliferator activated receptors (PPARs)

Peroxisome proliferator activated receptors (PPARs) belong to the superfamily of nuclear hormone receptors.[67] PPARs regulate gene expression by binding to specific DNA sequence elements within the promoter region of target genes called PPAR response elements (PPREs). When activated by their ligands, PPARs heterodimerize with retinoid X receptors, thereafter, bind to PPREs, and act as ligand-regulated transcription factors that control the expression of numerous genes involved in metabolic homeostasis, lipid and glucose metabolism, adipogenesis, inflammation, immunomodulation and bone metabolism.[68,69]

The PPARs are classified into three subtypes, PPARα, β/δ and γ. PPARγ has three variants; γ 1, 2 and 3. They are ubiquitously expressed, but have a tissue-specific distribution.[70-72]. PPARα is expressed in brown adipose tissue, liver, kidney, skeletal muscle, and bones. PPARβ/δ is expressed in many tissues but markedly in brain, adipose tissue, and skin. PPARγ is mostly found in adipose tissues, colon and macrophages. All PPAR subtypes are expressed in bone and skeletal muscle.[73,74]

PPARs bind to many ligands including monounsaturated fatty acids (MUFA), polyunsaturated fatty acids (PUFA) (ω-7 MUFA palmitoleic acid, oleic acid, ω-6 PUFA, ω-3 PUFAs), eicosanoids (arachidonic acid, docosahexaenoic acid and eicosapentaenoic acid), nonsteroidal inflammatory agents and a heterogeneous class of chemicals.[67,70,71,75]

PPARs act as regulators of glucose and lipid metabolism and also display anti-inflammatory effects.[76,77] Both PPARα[78] and PPARβ[79,80] are involved in fatty acid oxidation, whereas PPARγ[81] regulates energy storage and plays a role in adipocyte differentiation homeostasis. Accordingly, PPAR-α ligands such as fibrates are used for treatment of dyslipidemia due to their ability to lower plasma triglyceride levels and elevate HDL cholesterol levels.[82] Thiazolidinediones (TZDs) are the PPARγ agonists currently in use for the treatment of type 2 diabetes.[75] This treatment has, however, been questioned because several large clinical trials revealed an association between long-term therapy and increased risk of fracture.[83]

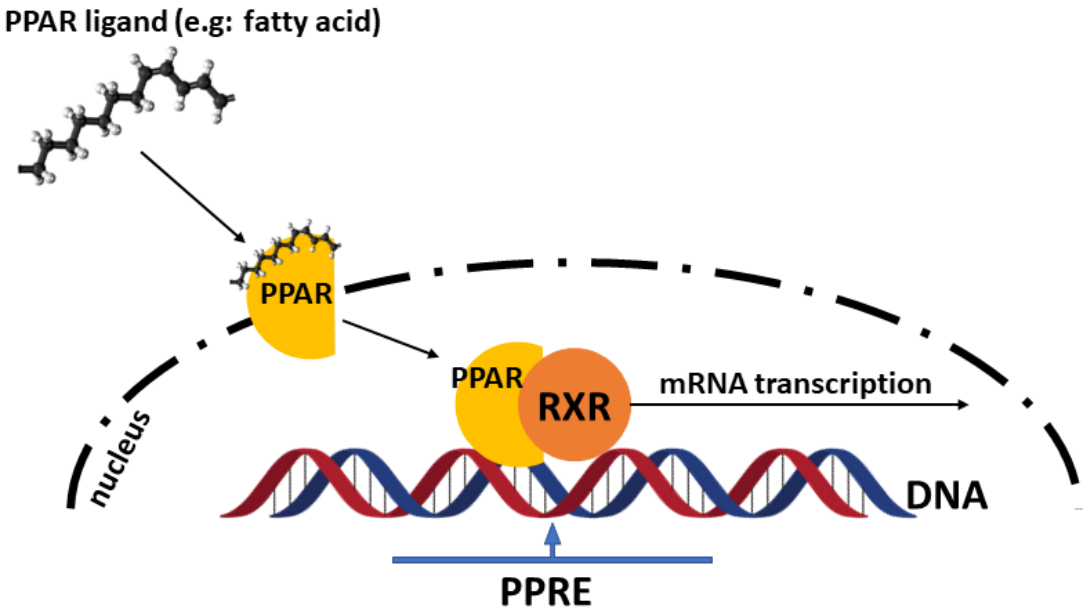

Figure 1.4: Mechanism of gene transcription by PPARs.

Upon activation by their ligands, PPARs heterodimerize with retinoid X receptors, thereafter, bind to PPREs, and act as ligand-regulated transcription factors that control the mRNA expression of numerous genes. The figure was modified from "Peroxisome Proliferator-Activated Receptor Family and Its Relationship to Renal Complications of the Metabolic Syndrome" by Guan et al.[84]

1.4.1. Peroxisome proliferator activated receptors and bone

All PPARs are involved in regulation of bone metabolism. PPARα activation facilitates differentiation of mesenchymal stem cells to osteoblasts rather than adipocytes by enhancing the receptor signaling of bone morphogenic proteins 4 and upregulating sirtuin 1 which in turn inhibits PPARγ.[85,86] Our research group has previously shown that the PPARα agonist

fenofibrate increases bone mineral density both in intact and ovariectomized osteoporotic female rats suggesting a positive impact on skeletal homeostasis.[73]

PPARβ/δ has also been shown to be a regulator of bone turnover and of the crosstalk between osteoclasts and osteoblasts. Scholtysek et al. found that activation of PPARβ/δ enhanced Wnt- and β-catenin dependent signaling, resulting in increased expression of OPG and inhibition of osteoclastogenesis. Accordingly, PPARβ/δ-deficient mice exhibited higher numbers of osteoclasts and osteopenia.[87] Moreover, PPARα/δ agonists such as bezafibrate and linoleic acid were shown to upregulate osteoblast differentiation and induce periosteal bone formation in intact male rats.[88]

PPARγ agonists affect bone negatively by directing MSCs towards adipocytes rather than osteoblasts. Moreover, TZDs have also been reported to inhibit bone formation by inducing osteocyte apoptosis and sclerostin upregulation.[89]

1.4.2. Peroxisome proliferator activated receptors and body weight

Our group and others have reported that PPARα agonists such as fenofibrate decrease fat mass and to promote weight loss in rodents and in rodent models of obesity.[73,90,91] There are several potential mechanisms for the weight loss including reduced appetite, increased fatty acid oxidation and increased energy expenditure. A combination of PPAR*α* and PPAR*δ* agonists (GW4148) has been reported to induce significant weight loss in animal models.[92] Garbacz et al. suggested that PPAR*δ* agonist induced weight loss requires PPAR*α* signaling.[93] On the other hand, PPARγ agonists induce weight gain in diabetic animals and patients with type 2 DM.[94,95]

1.4.3. Peroxisome proliferator activated receptors and lipocalin 2

Lipocalin 2 has been reported to be a selective modulator of PPARγ activation and function in lipid homeostasis and energy expenditure. On the other hand, administration of the TZD rosiglitazone to genetic obese mice has been shown to reduce lipocalin 2 gene expression in adipose tissue. Similarly, rosiglitazone exposure also induce a decline in lipocalin 2 mRNA expression in 3T3-L1 adipocytes.[96]

The PPAR pan agonists palmitate and oleate induced lipocalin 2 expression and secretion more significantly than eicosapentaenoic acid (EPA), a natural PPARα agonist, whereas phytanic acid, another PPAR pan agonist, significantly reduced lipocalin 2 protein expression and secretion after 24-hour treatment.[50]

There are no reports of the interplay between lipocalin 2 and PPARα agonists in osteoblast and osteocytes. Given the weight-reducing effect of fenofibrate, we aimed to explore

whether this could be mediated through stimulation of lipocalin 2 release from osteoblasts and osteocytes in vitro. Moreover, we had access to plasma samples from rats exposed to fenofibrate for two months, enabling assessment of the effect on plasma lipocalin 2 level under in vivo conditions.

2. Hypothesis

We hypothesize that PPAR alpha agonist fenofibrate exerts its weight-reducing effect partly through stimulation of lipocalin 2 release.

3. Research Aims

i. To study the effect of fenofibrate on the expression and release of lipocalin 2 from cells of the osteoblastic lineages MC3T3-E1 and MLO-Y4.

ii. To study the effect of fenofibrate on plasma levels of lipocalin 2 in ovariectomized rats.

4. Materials and Methods

4.1. Cell lines

The MC3T3-E1 and MLO-Y4 cell lines were used during the experimental work. The pre-osteoblastic MC3T3-E1 cell line was purchased from American Type Culture Collection (ATCC). This cell line was established from C57BL/6 mouse calvaria and selected based on high ALP- activity in the resting state. The cells have the capacity to differentiate into osteoblasts and osteocytes and have been demonstrated to form calcified bone matrix in vitro.[97]

The MLO-Y4 cell line was kindly provided by Lynda F. Bonewald (University of Missouri–Kansas City, USA). This murine cell line was established from transgenic mice created using the osteocalcin promoter which was transfected into the osteoblast using large T antigen.[98]

4.2. Basal culture conditions

4.2.1. MC3T3-E1 cell line

The MC3T3-E1 cells were cultured in Minimal Essential Medium-alpha (MEM-alpha) (Gibco) supplemented with 10% FCS (Sigma-Aldrich), 100 µg/mL penicillin/100 µg/mL streptomycin (Gibco), 100 mM sodium pyruvate (Gibco), 0.1 mg/ml fungizone (Gibco) and 1% glutamine (Gibco). The cells were grown in a monolayer in 75cm^2 culture flasks; 200,000 cells were seeded in 10 mL culture medium. The cells were sub-cultured twice a week. In each subculture, the cells were briefly rinsed with three ml 0.05% Trypsin/ 0.5 mM EDTA solution (Sigma-Aldrich) to remove all traces of serum followed by 2.5 ml of Trypsin-EDTA solution to flask and incubated at 37°C. After 3-3.5 minutes, the cells were observed under an inverted microscope to check for dispersion. 7.5 ml medium was added to the cells to stop trypsinization and then aspirated by gentle pipetting. Then the cell suspension was centrifuged for five minutes at 480 xg. The supernatant was discarded, and the cell pellet was re-suspended in one ml medium. Ten ml new medium was added to new culture flasks along with appropriate aliquots of the cell suspension.

4.2.2. MLO-Y4 cell line

The MLO-Y4 cell line was cultured in MEM-alpha (Gibco) supplemented with 5% FCS (Sigma-Aldrich), 5% fetal bovine serum (Sigma-Aldrich), 100 µg/mL penicillin/100 µg/mL streptomycin (Gibco), 100 mM sodium pyruvate (Gibco), 0.1 mg/ml fungizone (Gibco) and 1% glutamine (Gibco). The cells were cultured on Rat tail type I collagen (Becton Dickson Bioscience) coated flasks. Collagen was diluted in sterile 0.02 M acetic acid to a final

concentration of 0.15 mg/ml. A chilled pipet was used to avoid sticking of collagen to the pipet wall. Eight ml collagen solution was used to coat 75 cm^2 culture flasks and two ml/well collagen solution was used to coat six-well plates. After one hour at room temperature (inside hood), the plates were tilted for several minutes to remove excess collagen. To use immediately, the plates were rinsed with PBS to remove residual acid. Prior to storage at 4°C, the plates were left with the lid off inside the hood for minimum one hour to completely dry the plates.

MLO-Y4 cells were grown in a monolayer in 75 cm^2-culture flasks; 100,000 cells were seeded in ten mL medium. The cells were sub-cultured twice a week. In each subculture, the cells were briefly rinsed with three ml a 0.05% Trypsin/ 0.5 mM EDTA solution (Sigma-Aldrich) to remove all traces of serum followed by three ml of Trypsin-EDTA solution to flask and incubated at 37°C. After 3-3.5 minutes, the cells were observed under an inverted microscope to check for dispersion. Seven ml medium was added to the cells to stop trypsinization and then aspirated by gentle pipetting. Then the cell suspension was centrifuged for five minutes at 120xg. The supernatant was discarded, and the cell pellet was re-suspended in one ml medium. A mixture of conditioned medium from the previous culture and new medium was added to previously collagen-coated culture flasks along with appropriate aliquots of the cell suspension.

Both cell lines were incubated in an incubator at 37°C with an atmosphere of 5% CO_2 in humidified air. The growth medium and trypsin/EDTA were preheated to 37°C before use.

4.3. Cell counting

Cells were counted in a Countess automated cell counter (Invitrogen). A ten µl sample of cell suspension was mixed with ten µl of trypan blue, and then ten µl of this mixture was added to the slide. Viability (usually between 90-99%) and the number of live, dead and total cells could then be calculated. Cell counting was performed prior to sub-culturing the cells and before experiments.

4.4. Experimental conditions

4.4.1. Exposure to fenofibrate

Stock fenofibrate (MW 360.83 g/mol) solution (10 mM) (Sigma-Aldrich) was made by adding 20 mg fenofibrate in 5.54 ml dimethyl sulfoxide (DMSO) (Sigma-Aldrich). Ten µM fenofibrate solution was made by adding 50 µl stock in 50 ml medium (1% FCS). Then, one µM fenofibrate

was made by adding 5 ml of 10 µM fenofibrate solution in 45 ml medium (1% FCS). DMSO was used as control. 50 µl DMSO (Stock solution) was added in 50 ml medium (1% FCS) to make 1% DMSO in medium. Then, five ml of 1% DMSO was added to 45 ml medium (1% FCS) to make 0.1% DMSO in medium solution.

The MC3T3-E1 cells used in the experiments were from passage 18-24. The cells were seeded in six-well plates at a concentration of 200,000 cells/well and cultured for 24 hours. After 24 hours, old medium was discarded, and cells were exposed to fenofibrate (10 µM) solution in medium (1% FCS) for 24 and 72 hours. Cells were cultured in parallel in DMSO control solution (1%) in medium (1% FCS). The medium from the flasks were collected into separate Eppendorf tubes and kept at -20°C pending ELISA analyses.

The MLO-Y4 cells used in the experiments were from passage 17-34. The cells were seeded in six-well plates at a concentration of 100,000 cells/well and cultured for 48 hours. After 48 hours, old medium was discarded, and cells were exposed fenofibrate (1 and 10 µM) solutions in medium (1% FCS) for 24 and 72 hours. Cells were cultured in parallel in DMSO control solutions (0.01% and 0.1%) in medium (1% FCS). The medium from the six well plates were collected into separate Eppendorf tubes and kept at -20°C before ELISA analyses.

4.4.2. Protein extraction

Cell lysis buffer was made by carefully mixing 150 mM NaCl (Sigma-Aldrich), 50 mM tris-Cl (Sigma-Aldrich), 1% NP40 (Sigma-Aldrich), 10% Glycerol (Sigma-Aldrich), one tablet Protease inhibitor (Sigma-Aldrich), and 6.9 ml water. The lysis buffer was aliquoted (447 µl /epp. Tube) and stored at -20°C. Lysis buffer was mixed with 50 µl NaF (0.5 M) (Sigma-Aldrich) and 2.5 µl Na3VO4 (200 mM) (Sigma-Aldrich) to a total volume of approximately 500 µl).

Each well of MC3T3-E1 cells was washed with 0.5 ml Trypsin-EDTA solution, then cells were detached using 0.5 ml Trypsin-EDTA solution, before two ml medium was added to each well and carefully collected into separate Eppendorf tubes and centrifuged for five minutes at 480 xg. The tubes were put on ice while removing the medium and resuspending cell pellets with one ml cold PBS (4°C) (Sigma-Aldrich), and transferring to new Eppendorf tubes. The cell solutions were centrifuged again for two minutes at 625 xg at 4°C and the PBS wash was repeated with 0.5 ml PBS. Supernatants were removed and discarded carefully. The cell pellets were left on ice for 20-30 minutes after adding lysis buffer to each sample (20 µl for 0.5 million cells/well sample) and mixed by pipetting up and down a few times. Then, the lysates were centrifuged at 800 xg for 15 minutes at 4°C. The supernatant was transferred to

new Eppendorf tubes, the pellet was discarded. Finally, the samples were stored at -80°C until protein estimation.

MLO-Y4 cells were gently washed by cold PBS twice. 200 µl lysis buffer was added to each well and the bottom of the wells were scraped with cell scraper. Then, the samples were collected into separate Eppendorf tubes and kept on ice for 20-30 minutes, before it was centrifuged at 800 xg for 15 minutes at 4°C. The supernatants were transferred to new Eppendorf tubes, and the pellets were discarded. Finally, the samples were stored at -80°C pending protein estimation.

4.4.3. Total protein measurements

Cell lysates collected earlier as described above were retrieved from the -80°C freezer and put on ice. All samples were diluted 1:100. The diluted lysates were kept on ice to protect proteins from heat-induced denaturation. Then the total protein was quantified from the lysates using 96 well plate (Corning) and Micro BSA protein assay kit (Thermo Fischer) following the manufacturer's protocol. BSA protein dilutions for the standard curve were prepared according to the protocol as described in Table 4.1.

Table 4.1: Standard curve for protein concentration (micro BSA protein assay kit)

Tube	PBS (µl)	BSA (µl)	BSA tube	µg/ml [BSA]	Total volume (µl)
A	665	35	Stock	100	700
B	350	350	A	50	700
C	350	350	B	25	700
D	350	350	C	12,5	700
E	350	350	D	6,25	700
F	350	350	E	3,125	700
G	200	200	F	1,56	400
Blank	350	-	-	0	350

Firstly, the standard solution and samples were added 100 µl/well. Working Reagent (WR) solution was made as described in the kit protocol. MA, MB and MC reagents were mixed respectively following 25:24:1 ratio. Then, WR solution was added (100 µl/well) and then incubated at 37°C for two hours.

An iMark™ microplate reader (Bio-Rad, California, US) was used for absorbance measurements at 570 nm. The amount of protein was then estimated using the Microplate Manager 6.0 (MPM 6.0) (Biorad, California, USA) software program.

4.4.4. Lipocalin 2 measurements

Lipocalin 2 concentrations in the protein extract and culture medium were determined using a Rat Lipocalin-2/NGAL Duoset ELISA Kit (R&D Systems, Minneapolis, USA) following the manufacturer's protocol. The standard curve was made according to the manufacturer's instructions, except that 20 pg/ml standard was mixed with one ml reagent diluent instead of five pg/ml to produce an optimal standard curve. Cell lysates were diluted 1:100 and medium was diluted 1:50. An iMark™ microplate reader (Bio-Rad, US) was used for absorbance measurements at 450 nm subtracted from 570 nm. The amount of lipocalin 2 was then estimated using Microplate Manager 6.0 (MPM 6.0) (Biorad, California, USA) software program.

4.4.5. RNA isolation

The MLO-Y4 cells were seeded and exposed to fenofibrate and control solutions as described earlier. Total RNA isolation was done following the RNeasy kit protocol. Lysis buffer was made by mixing ten µl β-mercaptoethanol with each ml of RLT lysis buffer following protocol. medium from the six well plates were discarded, and the wells were gently washed by cold PBS twice. 350 µl lysis buffer was added to each well and the bottom of the wells were scraped with cell scraper. Then, the cell lysates were collected into separate Eppendorf tubes and kept on ice. The cell lysates were homogenized using a syringe and needle. Lysates were passed through a 20-gauge (0.9 mm) needle attached to a sterile plastic syringe at least 5–10 times until a homogeneous lysate was achieved. The concentration of the extracted total RNA was measured by the Nanodrop® ND-1000 Spectrophotometer (Thermo Scientific, Massachusetts, United States). Finally, the lysates were stored at -80°C pending complementary DNA (cDNA) synthesis.

4.4.6. cDNA synthesis

Isolated total single stranded RNA from MLO-Y4 cells was converted to more stable double-stranded cDNA before the polymerase chain reaction (PCR). cDNA synthesis was performed using the Thermo Scientific Maxima First Strand cDNA synthesis kit for real time quantitative PCR (RT-qPCR) (Thermo Scientific, Massachusetts, United States). cDNA was made from 500 ng mRNA and the total reaction volume was 20 µL per RNA sample. Each reaction was

prepared as described in Table 4.2. The. Samples were then mixed gently and incubated for ten minutes at room temperature, followed by 15 minutes at 50°C and finally five minutes at 85°C to stop the reaction. Two µl from each cDNA sample were pooled into a tube to use for the relative standard curve and dilution were done with nuclease-free water in serial dilution: 1. 0.5, 1, 0.5, 0.2, 0.1, 0.05, 0.02, 0.01 and 0.005. Thereafter, all cDNA samples were diluted 1:2 in nuclease-free water, and samples and relative standards were stored at -20°C pending qPCR.

Table 4.2: cDNA synthesis reaction setup

Component	Volume/amount per reaction
5x reaction mix	4 µL
Maxima enzyme mix	2 µL
RNA sample	500 ng
Nuclease free water	Up to a total of 20 µL

4.4.7. Quantitative polymerase chain reaction (qPCR)

qPCR was performed to assess the relative mRNA expression lipocalin 2 in MLO-Y4 cells following protocol. The primers and probes for lipocalin 2 and housekeeping gene glyceraldehyde-3-phosphate dehydrogenase (GAPDH) were purchased from Thermo Scientific, Massachusetts, United States. And are shown in Table 4.3. Glyceraldehyde 3-phosphate dehydrogenase (GAPDH) was used as a reference gene, and lipocalin 2 expression was normalized to GAPDH for correction of variations in amount of RNA in the samples.

Table 4.3: Primer information for genes used in qPCR reaction

Target genes	Forward sequence (5’ to 3’)	Reverse sequence (3’ to 5’)	Species	Sequence ID
GAPDH	GGTCCCAGCT TAGGTTCATCA	GAGATGCTCA GTGTTGGGGG	Mouse	NM_001289726.1
Lipocalin 2	GAACTTGATC CCTGCCCCAT	TGAACCATTG GGTCTCTGCG	Mouse	NM_008491.1

qPCR reaction mix containing PerfeCTa FastMix II with ROX (2x) (Quantabio, Beverly, USA) was made following the manufacturer’s instructions. The reaction mix is described in Table

4.4. The master mix and the primer/probe mix was added to 96-well qPCR plates. Standards were run in triplicates and samples were run in duplicates.

Table 4.4: qPCR reaction mix setup

Component	Volume
Primer/ probe mix	1 µL
PerfeCTa FastMix II with ROX (2x)	10 µL
Nuclease-free water	7 µL
Standard or sample	2 µL
Total volume of qPCR reaction mix	20 µL

qPCR was performed on a StepOnePlus™ Real-time PCR (Applied Biosystems, Foster City, CA) for amplification and quantification according to the protocol. At the holding stage, the parameters were set to 95°C (10 minutes). Afterwards, the parameters were set to 95°C (15 seconds) to denature double-stranded DNA (dsDNA) in the cycling stage followed by 60°C (60 seconds) for annealing and elongation of DNA.

4.5. In vivo study

4.5.1. Rat Plasma Sample

Sprague Dawley rats, 15 weeks old, were assigned to five groups as described earlier. One group was sham-operated and the others ovariectomized (OVX). Two of the OVX groups were given fenofibrate 90 mg/kg/day (Sigma-Aldrich, Norway), solely or combined with jumping exercise, using methylcellulose (M7140, Sigma-Aldrich, Norway) as vehicle. A third group underwent jumping exercise and vehicle administration. The Sham and OVX control groups were given vehicle only. Substances were administered by daily intragastric gavage for eight weeks. Blood samples were collected by cardiac puncture at termination, and plasma samples were stored at -80°C until analysis.

4.5.2. Analysis of lipocalin 2 in rat plasma

Lipocalin 2 concentrations in plasma samples from OVX controls and OVX rats given fenofibrate solely were determined using a Rat Lipocalin-2/NGAL Duoset ELISA Kit (R&D Systems, Minneapolis, USA) following the manufacturer's protocol. The standard curve was made following the manufacturer's instructions, except that 50 pg/ml standard was mixed with

one ml reagent diluent instead of five pg/ml to produce an optimum standard curve and the plasma samples were undiluted. An iMark™ microplate reader (Bio-Rad, California, US) was used for absorbance measurements at 450 nm subtracted from 570 nm. The amount of lipocalin 2 was then estimated using Microplate Manager 6.0 (MPM 6.0) (Biorad, California, USA) software program.

4.6. Statistical analysis

The data from fenofibrate and control treated groups were checked for normal distribution using Shapiro-Wilk test first. Depending on whether the data were normally distributed or not, unpaired two tailed student's T-test or Mann-Whitney test was performed. Results were considered statistically significant if p-values were less than 0.05 (*). Data were presented as mean ± standard error of mean (SEM). GraphPad Prism 8 (La Jolla, California, USA) was utilized to create graphs.

5. Results

5.1. Cell studies

5.1.1. Lipocalin 2 in MC3T3-E1 cells

As shown in Figure 5.1 and 5.2, no significant differences in lipocalin 2 levels in cell medium or cell lysate (corrected for total protein) from MC3T3-E1 cells were observed after incubation with fenofibrate 10 µM and control for 24 and 72 hours. The data are based on five experiments.

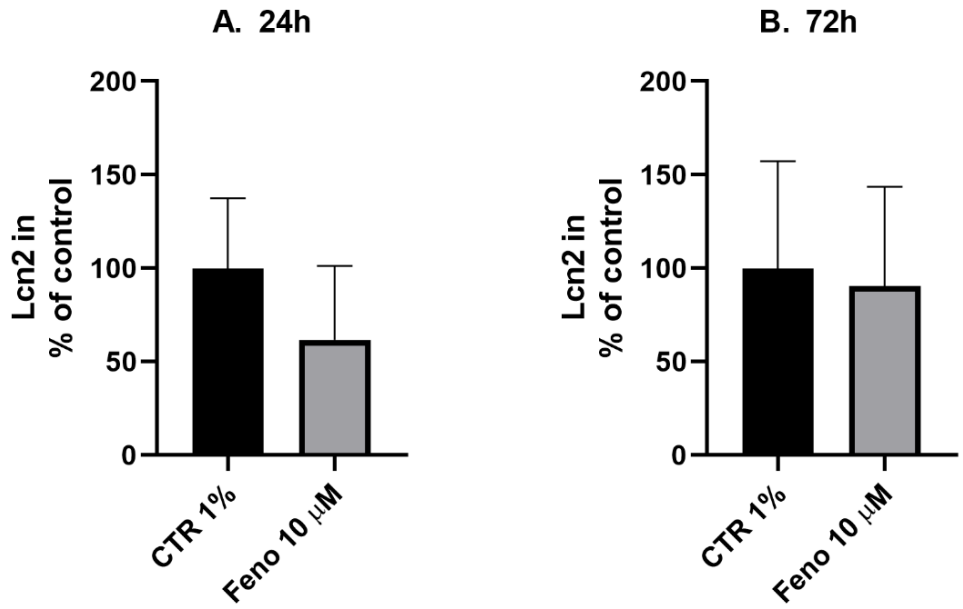

Figure 5.1: Lipocalin 2 concentration in medium from MC3T3-E1 cells, measured by ELISA.

Cells were incubated with DMSO 1% control and fenofibrate 10 µM dissolved in DMSO for 24 and 72 hours. Data are presented as mean ± SEM in % of control from two parallels and the figure represents data from five different experiments (n=5).

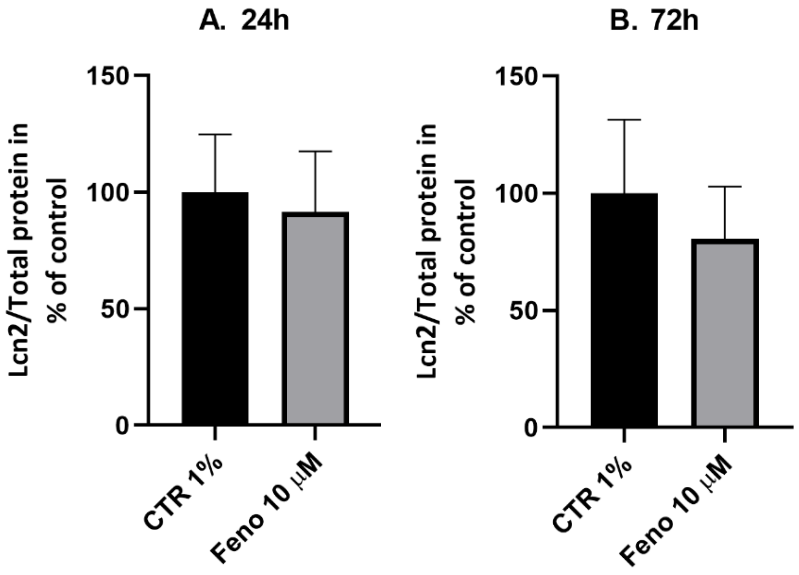

Figure 5.2: Lipocalin 2 concentration in cell lysate corrected for total protein concentration in MC3T3-E1 cells, measured by ELISA.

Cells were incubated with DMSO 1% control and fenofibrate 10 µM dissolved in DMSO for 24 and 72 hours. Data are presented as mean ± SEM in % of control from two parallels and the figure represents data from five different experiments (n=5).

5.1.2. Lipocalin 2 in MLO-Y4 cells

As shown in Figures 5.3A, 5.3B, 5.4A and 5.4B, no significant differences were observed in lipocalin 2 concentration in medium or cell lysate after 24 and 72 hours. After 72 hours, cells exposed to fenofibrate 1 µM appeared to secrete higher amount of lipocalin 2 both in medium and lysate, as well as cells exposed to fenofibrate 10µM compared to control. The data are based on three experiments. As shown in Appendix table 3 and 4, there was considerable variation in the levels between the different experiments.

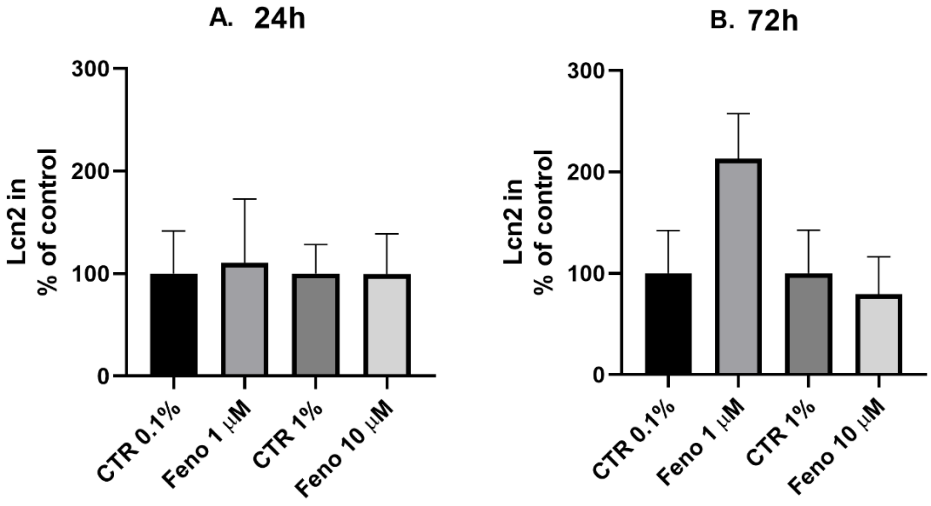

Figure 5.3: Lipocalin 2 concentration in medium by MLO-Y4 cells, measured by ELISA.

Cells were incubated with DMSO 1% control and fenofibrate 10 µM dissolved in DMSO for 24 and 72 hours. Data are presented as mean ± SEM in % of control from two parallels and the figure represents data from three different experiments (n=3).

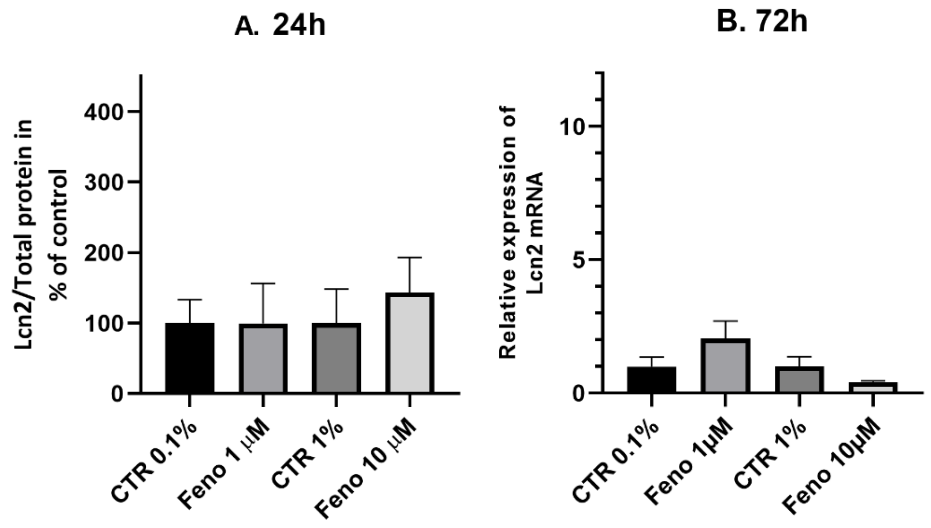

Figure 5.4: Lipocalin 2 concentration in cell lysate corrected for total protein concentration in MLO-Y4 cells, measured by ELISA.

Cells were incubated with DMSO 1% control and fenofibrate 10 µM dissolved in DMSO for 24 and 72 hours. Data are presented as mean ± SEM in % of control from two parallels and the figure represents data from three different experiments (n=3).

5.2. Lipocalin 2 mRNA expression in MLO-Y4 cells

As shown in figure 5.6A, the lipocalin 2 mRNA expression was highly and significantly upregulated by both 1 µM and 10 µM fenofibrate after 24 hours, although 1 µM stimulated more expression than 10 µM compared to control. After 72 hours, lipocalin 2 expression was lower in all samples than samples after 24 hours. Data from individual experiments are shown in Table 5.1. TNF α (1ng/ml and 0.1ng/ml) was used as a positive control as it is known to induce lipocalin 2 mRNA expression (not shown here).

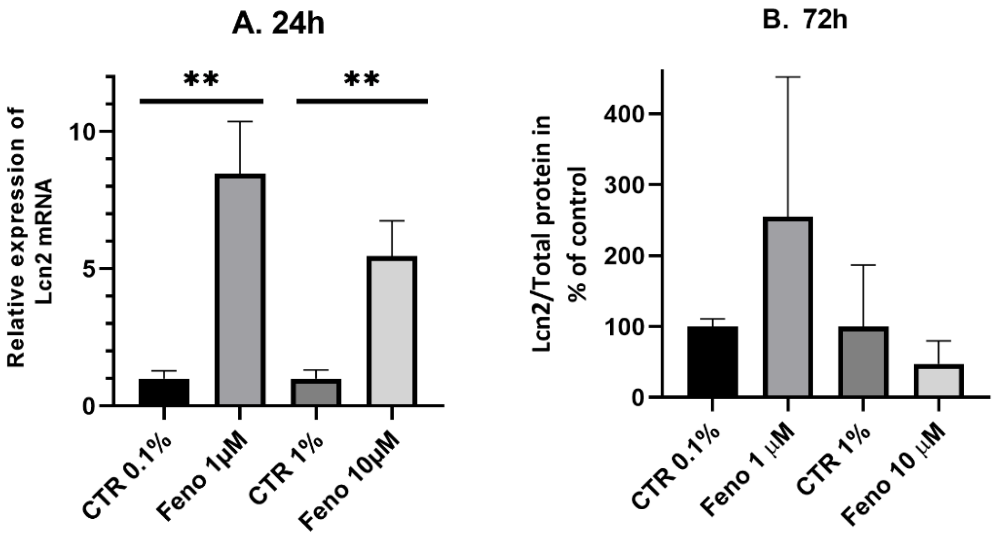

Figure 5.5: Lipocalin 2 mRNA expression in MLO-Y4 cells, measured by RTPCR.

Lipocalin 2 mRNA expression relative to housekeeping gene GAPDH was analyzed on samples from cells exposed to control (DMSO 0.1% and 1%) and fenofibrate (1 and 10 µM) dissolved in DMSO for 24 and 72 hours. Data are presented as mean ± SEM from three parallels and the figure represents data from two different experiments (n=2). The level of expression of lipocalin 2 mRNA is shown as fold changes relative to control.

Table 5.1: Individual biological replicates of relative expression of lipocalin 2 mRNA, measured by RTPCR.

Exposure time	Samples	Exp 1	Significance	Exp 2	Significance
24h	CTR 0.1%	1		1	
	Feno 1µM	7.913468107	**	10.70301471	**
	CTR 1%	1		1	
	Feno 10µM	5.316167709	**	5.998979754	-
72h	CTR 0.1%	1		1	
	Feno 1µM	1.958949628	**	2.776264252	-
	CTR 1%	1		1	
	Feno 10µM	0.29050779	*	1.309557506	-

Lipocalin 2 mRNA expression relative to housekeeping gene GAPDH was analyzed on samples from cells exposed to control (DMSO 0.1% and 1%) and fenofibrate (1 and 10 µM) dissolved in DMSO for 24 and 72 hours. The level of expression of lipocalin 2 mRNA is shown as fold changes relative to control. Data are presented as mean from three parallels of two different experiments (n=2). **$p<0.05$ = *, $p<0.01$ = **** significantly different compared to control.

5.3. In vivo study

5.3.1. Lipocalin 2 in Rat plasma

ELISA performed in duplicates from 12 rats in each group showed that plasma Lipocalin 2 level was higher, although not significant (Student's t test, p 0.11) in OVX rats exposed to fenofibrate compared to control (Figure 5.6).

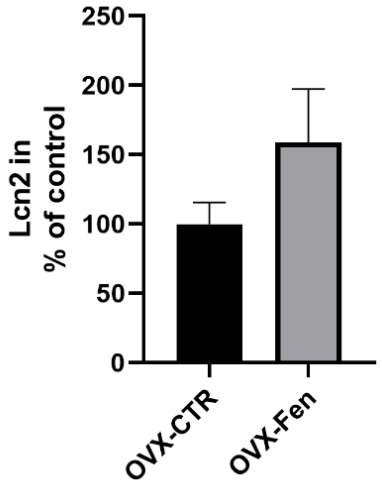

Figure 5.6: Plasma lipocalin 2 concentration in OVX rats.

OVX-Fen rat group was given fenofibrate 90 mg/kg/day using methylcellulose as vehicle and control group (OVX-CTR) was exposed to methylcellulose only for eight weeks. Data are presented as mean ± SEM in % of control and the figure represents data from 12 rats (n=12).

6. Discussion

Here we show for the first time the transcription, translation, and secretion of lipocalin 2 from the murine osteocyte cell line MLO-Y4. Moreover, we found that the PPARα agonist fenofibrate increased the mRNA expression of lipocalin 2 in a time- and dosage-dependent manner. Fenofibrate also seemed to enhance the release of lipocalin 2 from MLO-Y4 cells, albeit not significantly. Lipocalin 2 secretion from the pre-osteoblast cell line was modest and did not differ between fenofibrate-exposed cells and controls. Finally, circulating lipocalin 2 levels tended to be higher in OVX rats exposed to fenofibrate compared to controls.

Lipocalin 2 was previously referred to as an adipokine as it was considered to be exclusively released by adipocytes.[50] However, Mosaliou et al. demonstrated the expression of lipocalin 2 in murine osteoblasts, and reported a 10-fold higher expression in bone than in fat or any other tissue.[56] In the present study, we show that lipocalin 2 also is expressed in the osteocytes, which represent the end-stage of osteoblastic lineage. On the other hand, lipocalin 2 secretion from MC3T3-E1 pre-osteoblasts was scarce, indicating that differentiation is necessary for osteoblasts to express lipocalin 2.his is in accordance with Costa et al. who found that lipocalin 2 was expressed during osteoblast differentiation.[55]

Mosialou et al. showed that bone-derived lipocalin 2 suppressed appetite by binding to MC4R in hypothalamus.[56] This observation inspired us to explore whether substances known to lower body weight like fenofibrate exerted this effect through lipocalin 2. Intriguingly, lipocalin 2 mRNA expression was highly and significantly upregulated in MLO-Y4 osteocytes after 24 hours incubation with fenofibrate. Both concentrations of fenofibrate (1 and 10 µM) induced an increase in lipocalin 2 expression. The level of lipocalin 2 appeared to be higher in medium and lysate from MLO-Y4 cells exposed to fenofibrate 1 µM for 72 hours, however, not significant compared to control.

Osteocyte derived signals have been proposed to play a role in regulation of obesity. Jansson et al. showed that regulation of body weight may be orchestrated by the osteocytes of weight-bearing bones acting as a gravitostat. They did, however, not succeed to identify the anorexigenic factor.[99] Based on our findings, we speculate whether lipocalin 2 may be responsible for regulation of body weight by osteocytes.

To explore the effect of fenofibrate on lipocalin 2 in vivo, we measured plasma levels of lipocalin 2 in OVX rats exposed to fenofibrate for 8 weeks. Notably, OVX rats receiving fenofibrate displayed lower fat mass, higher lean mass and higher BMD than OVX controls.[73] Lipocalin levels tended to be higher in these rats than in OVX controls. Interestingly, OVX rats given fenofibrate in combination with jumping exercise displayed significantly higher

circulating lipocalin 2 levels than OVX controls (data not shown). It should be recalled that blood samples were drawn more than 24 hours after the last dosage of fenofibrate was given, and this may have attenuated the response.

The findings of this study support our hypothesis that lipocalin 2 may play a role in fenofibrate-induced weight loss.

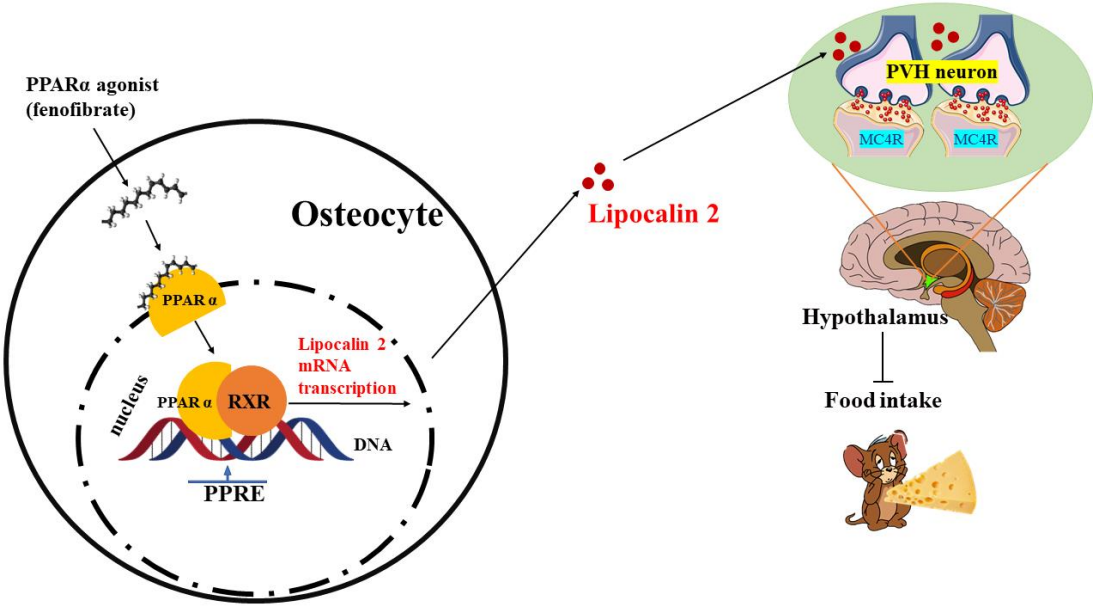

Figure 6.1: Hypothesis on weight-reducing effect of fenofibrate through osteocyte derived lipocalin 2.

Lipocalin 2 is expressed from osteocytes in response to fenofibrate and lowers appetite by binding to MC4R in hypothalamus. The figure was created based on the result from this experiment and "MC4R-dependent suppression of appetite by bone-derived lipocalin 2" by Mosialou et al.

The function of osteocytes has been difficult to explore since these cells are embedded in mineralized tissue and thus difficult to obtain in reasonable numbers and purity. Establishment of osteocyte cell lines has enabled studies of osteocyte function. In the present study we applied the murine osteocyte-like cell line MLO-Y4 cells derived from long bones.[98] These cells are representative of early, mature osteocytes and have been shown to be useful for studying osteocytes in vitro. However, they do not provide information on the alterations in gene expression and morphology that occur as osteoblasts differentiate into osteocytes.[98] Several osteoblastic cell lines have been reported to differentiate toward an osteocyte-like phenotype in culture, including HOB-01-C1 pre-osteocyte cells, MLO-A5 late osteoblast cells, and IDG-SW3 late osteoblast cells.[98] These in vitro models represent important tools in addition to in vivo models.

7. Limitations

There was considerable variation in lipocalin levels between the different cell experiments which may have impeded the possibility to show significant differences. Due to time constraints, more biological replicates could not be included and the effect of fenofibrate on lipocalin 2 expression and release could not be studied with more concentrations and exposure times.

8. Conclusion

We have for the first time shown that lipocalin 2 is expressed, translated and secreted from MLO-Y4 osteocytes, and that the expression of lipocalin 2 mRNA is significantly upregulated by the PPARα agonist fenofibrate. Our findings suggest that the fenofibrate-induced weight loss may be mediated by lipocalin 2. Moreover, our data add new knowledge concerning the endocrine role of the skeleton.

9. Future plans

1. Perform more studies on osteocytes to confirm our findings concerning fenofibrate.
2. Study the effect of other PPAR agonists on regulation of lipocalin 2 in MLO-Y4 osteocytes and in vivo (OVX rats).
3. Study the effect on lipocalin 2 in vitro and in (OVX rats, humans) of other weight-reducing agents such as metformin.
4. Study whether shear stress affects lipocalin 2 expression in MLO-Y4 cells.
5. Study the effect of exercise (rats and humans) on circulating lipocalin 2.

10. References

1. Han, Y., You, X., Xing, W., Zhang, Z. & Zou, W. Paracrine and endocrine actions of bone-the functions of secretory proteins from osteoblasts, osteocytes, and osteoclasts. *Bone Res* **6**, 16 (2018).
2. Mizokami, A., Kawakubo-Yasukochi, T. & Hirata, M. Osteocalcin and its endocrine functions. *Biochem Pharmacol* **132**, 1-8 (2017).
3. Feng, X. & McDonald, J.M. Disorders of bone remodeling. *Annu Rev Pathol* **6**, 121-145 (2011).
4. Buckwalter, J.A., Glimcher, M.J., Cooper, R.R. & Recker, R. Bone biology. I: Structure, blood supply, cells, matrix, and mineralization. *Instr Course Lect* **45**, 371-386 (1996).
5. Florencio-Silva, R., Sasso, G.R., Sasso-Cerri, E., Simões, M.J. & Cerri, P.S. Biology of Bone Tissue: Structure, Function, and Factors That Influence Bone Cells. *Biomed Res Int* **2015**, 421746 (2015).
6. Zoch, M.L., Clemens, T.L. & Riddle, R.C. New insights into the biology of osteocalcin. *Bone* **82**, 42-49 (2016).
7. Crockett, J.C., Rogers, M.J., Coxon, F.P., Hocking, L.J. & Helfrich, M.H. Bone remodelling at a glance. *J Cell Sci* **124**, 991-998 (2011).
8. Sugiyama, T., Price, J.S. & Lanyon, L.E. Functional adaptation to mechanical loading in both cortical and cancellous bone is controlled locally and is confined to the loaded bones. *Bone* **46**, 314-321 (2010).
9. Holtrop, M.E. & King, G.J. The ultrastructure of the osteoclast and its functional implications. *Clin Orthop Relat Res*, 177-196 (1977).
10. H.K, V., Y.-k, L., Lehenkari, P. & Uemara, T. How do osteoclasts resorb bone? *Materials Science and Engineering: C* **6**, 205-209 (1998).
11. Ugarte, F. & Forsberg, E.C. Haematopoietic stem cell niches: new insights inspire new questions. *Embo j* **32**, 2535-2547 (2013).
12. Kusumbe, A.P., Ramasamy, S.K. & Adams, R.H. Coupling of angiogenesis and osteogenesis by a specific vessel subtype in bone. *Nature* **507**, 323-328 (2014).
13. Suchacki, K.J*., et al.* Skeletal energy homeostasis: a paradigm of endocrine discovery. *J Endocrinol* **234**, R67-r79 (2017).
14. Kong, Y.Y*., et al.* OPGL is a key regulator of osteoclastogenesis, lymphocyte development and lymph-node organogenesis. *Nature* **397**, 315-323 (1999).
15. Lacey, D.L*., et al.* Osteoprotegerin ligand is a cytokine that regulates osteoclast differentiation and activation. *Cell* **93**, 165-176 (1998).
16. Yasuda, H*., et al.* Osteoclast differentiation factor is a ligand for osteoprotegerin/osteoclastogenesis-inhibitory factor and is identical to TRANCE/RANKL. *Proc Natl Acad Sci U S A* **95**, 3597-3602 (1998).
17. Simonet, W.S*., et al.* Osteoprotegerin: a novel secreted protein involved in the regulation of bone density. *Cell* **89**, 309-319 (1997).
18. Tsuda, E*., et al.* Isolation of a novel cytokine from human fibroblasts that specifically inhibits osteoclastogenesis. *Biochem Biophys Res Commun* **234**, 137-142 (1997).
19. Yasuda, H*., et al.* Identity of osteoclastogenesis inhibitory factor (OCIF) and osteoprotegerin (OPG): a mechanism by which OPG/OCIF inhibits osteoclastogenesis in vitro. *Endocrinology* **139**, 1329-1337 (1998).
20. Myers, D*., et al.* Expression of functional RANK on mature rat and human osteoclasts. *FEBS letters* **463**, 295-300 (1999).
21. Theoleyre, S*., et al.* The molecular triad OPG/RANK/RANKL: involvement in the orchestration of pathophysiological bone remodeling. *Cytokine Growth Factor Rev* **15**, 457-475 (2004).
22. Westendorf, J.J., Kahler, R.A. & Schroeder, T.M. Wnt signaling in osteoblasts and bone diseases. *Gene* **341**, 19-39 (2004).

23. Winkler, D.G.*, et al.* Osteocyte control of bone formation via sclerostin, a novel BMP antagonist. *Embo j* **22**, 6267-6276 (2003).
24. Huang, J.*, et al.* Crosstalk between MLO-Y4 osteocytes and C2C12 muscle cells is mediated by the Wnt/β-catenin pathway. *JBMR Plus* **1**, 86-100 (2017).
25. Greenblatt, M.B., Tsai, J.N. & Wein, M.N. Bone Turnover Markers in the Diagnosis and Monitoring of Metabolic Bone Disease. *Clin Chem* **63**, 464-474 (2017).
26. Autosomal dominant hypophosphataemic rickets is associated with mutations in FGF23. *Nat Genet* **26**, 345-348 (2000).
27. Shimada, T.*, et al.* Targeted ablation of Fgf23 demonstrates an essential physiological role of FGF23 in phosphate and vitamin D metabolism. *J Clin Invest* **113**, 561-568 (2004).
28. Andrukhova, O.*, et al.* FGF23 acts directly on renal proximal tubules to induce phosphaturia through activation of the ERK1/2-SGK1 signaling pathway. *Bone* **51**, 621-628 (2012).
29. Huang, X., Jiang, Y. & Xia, W. FGF23 and Phosphate Wasting Disorders. *Bone Res* **1**, 120-132 (2013).
30. Bergwitz, C. & Jüppner, H. Regulation of phosphate homeostasis by PTH, vitamin D, and FGF23. *Annu Rev Med* **61**, 91-104 (2010).
31. Ducy, P.*, et al.* Increased bone formation in osteocalcin-deficient mice. *Nature* **382**, 448-452 (1996).
32. Otani, T.*, et al.* Signaling pathway for adiponectin expression in adipocytes by osteocalcin. *Cell Signal* **27**, 532-544 (2015).
33. Mera, P.*, et al.* Osteocalcin signaling in myofibers is necessary and sufficient for optimum adaptation to exercise. *Cell metabolism* **23**, 1078-1092 (2016).
34. Ferron, M., Hinoi, E., Karsenty, G. & Ducy, P. Osteocalcin differentially regulates β cell and adipocyte gene expression and affects the development of metabolic diseases in wild-type mice. *Proceedings of the National Academy of Sciences* **105**, 5266-5270 (2008).
35. Lee, N.K.*, et al.* Endocrine regulation of energy metabolism by the skeleton. *Cell* **130**, 456-469 (2007).
36. Oury, F.*, et al.* Endocrine regulation of male fertility by the skeleton. *Cell* **144**, 796-809 (2011).
37. Oury, F.*, et al.* Maternal and offspring pools of osteocalcin influence brain development and functions. *Cell* **155**, 228-241 (2013).
38. Xia, M.*, et al.* Influence of serum osteocalcin and liver fat content on glucose metabolism in a middle-aged and elderly Chinese population. in *DIABETOLOGIA*, Vol. 57 S122-S122 (SPRINGER 233 SPRING ST, NEW YORK, NY 10013 USA, 2014).
39. Ferron, M.*, et al.* Insulin signaling in osteoblasts integrates bone remodeling and energy metabolism. *Cell* **142**, 296-308 (2010).
40. Lacombe, J., Karsenty, G. & Ferron, M. In vivo analysis of the contribution of bone resorption to the control of glucose metabolism in mice. *Molecular metabolism* **2**, 498-504 (2013).
41. Ferron, M. & Lacombe, J. Regulation of energy metabolism by the skeleton: osteocalcin and beyond. *Archives of biochemistry and biophysics* **561**, 137-146 (2014).
42. Mera, P., Ferron, M. & Mosialou, I. Regulation of energy metabolism by bone-derived hormones. *Cold Spring Harbor perspectives in medicine* **8**, a031666 (2018).
43. Oury, F.*, et al.* Osteocalcin regulates murine and human fertility through a pancreas-bone-testis axis. *The Journal of clinical investigation* **123**, 2421-2433 (2013).
44. Berger, J.M.*, et al.* Mediation of the Acute Stress Response by the Skeleton. *Cell Metab* **30**, 890-902.e898 (2019).
45. Kanazawa, I. Osteocalcin as a hormone regulating glucose metabolism. *World J Diabetes* **6**, 1345-1354 (2015).
46. Lögdberg, L. & Wester, L. Immunocalins: a lipocalin subfamily that modulates immune and inflammatory responses. *Biochimica et Biophysica Acta (BBA)-Protein Structure and Molecular Enzymology* **1482**, 284-297 (2000).

47. Flo, T.H*., et al.* Lipocalin 2 mediates an innate immune response to bacterial infection by sequestrating iron. *Nature* **432**, 917-921 (2004).
48. Kjeldsen, L., Bainton, D.F., Sengelov, H. & Borregaard, N. Identification of neutrophil gelatinase-associated lipocalin as a novel matrix protein of specific granules in human neutrophils. (1994).
49. Lu, F., Inoue, K., Kato, J., Minamishima, S. & Morisaki, H. Functions and regulation of lipocalin-2 in gut-origin sepsis: a narrative review. *Critical Care* **23**, 269 (2019).
50. Zhang, Y*., et al.* Lipocalin 2 expression and secretion is highly regulated by metabolic stress, cytokines, and nutrients in adipocytes. *PloS one* **9**(2014).
51. Cowland, J.B. & Borregaard, N. Molecular characterization and pattern of tissue expression of the gene for neutrophil gelatinase-associated lipocalin from humans. *Genomics* **45**, 17-23 (1997).
52. Friedl, A., Stoesz, S., Buckley, P. & Gould, M. Neutrophil gelatinase-associated lipocalin in normal and neoplastic human tissues. Cell type-specific pattern of expression. *The Histochemical journal* **31**, 433-441 (1999).
53. Huang, H., Chu, S. & Chen, Y. Ovarian steroids regulate 24p3 expression in mouse uterus during the natural estrous cycle and the preimplantation period. *Journal of Endocrinology* **162**, 11-19 (1999).
54. Zhang, J*., et al.* The role of lipocalin 2 in the regulation of inflammation in adipocytes and macrophages. *Molecular endocrinology* **22**, 1416-1426 (2008).
55. Costa, D*., et al.* Altered bone development and turnover in transgenic mice over-expressing lipocalin-2 in bone. *Journal of cellular physiology* **228**, 2210-2221 (2013).
56. Mosialou, I*., et al.* MC4R-dependent suppression of appetite by bone-derived lipocalin 2. *Nature* **543**, 385-390 (2017).
57. Shen, F. Hu Z, Goswami J, Gaffen SL. *Identification of common transcriptional regulatory elements in interleukin-17 target genes. J Biol Chem* **281**, 24138-24148 (2006).
58. Sommer, G*., et al.* Lipocalin-2 is induced by interleukin-1β in murine adipocytes in vitro. *Journal of cellular biochemistry* **106**, 103-108 (2009).
59. Roudkenar, M.H*., et al.* Lipocalin 2 regulation by thermal stresses: protective role of Lcn2/NGAL against cold and heat stresses. *Experimental cell research* **315**, 3140-3151 (2009).
60. Garay-Rojas, E., Harper, M., Hraba-Renevey, S. & Kress, M. An apparent autocrine mechanism amplifies the dexamethasone-and retinoic acid-induced expression of mouse lipocalin-encoding gene 24p3. *Gene* **170**, 173-180 (1996).
61. Roudkenar, M.H*., et al.* Oxidative stress induced lipocalin 2 gene expression: addressing its expression under the harmful conditions. *Journal of radiation research* **48**, 39-44 (2007).
62. Zhao, P. & Stephens, J.M. STAT1, NF-κB and ERKs play a role in the induction of lipocalin-2 expression in adipocytes. *Molecular Metabolism* **2**, 161-170 (2013).
63. Seth, P*., et al.* Cellular and molecular targets of estrogen in normal human breast tissue. *Cancer Res* **62**, 4540-4544 (2002).
64. Capulli, M*., et al.* A Complex Role for Lipocalin 2 in Bone Metabolism: Global Ablation in Mice Induces Osteopenia Caused by an Altered Energy Metabolism. *J Bone Miner Res* **33**, 1141-1153 (2018).
65. Rucci, N*., et al.* Lipocalin 2: a new mechanoresponding gene regulating bone homeostasis. *J Bone Miner Res* **30**, 357-368 (2015).
66. Paton, C.M*., et al.* Lipocalin-2 increases fat oxidation in vitro and is correlated with energy expenditure in normal weight but not obese women. *Obesity (Silver Spring)* **21**, E640-648 (2013).
67. Schoonjans, K., Martin, G., Staels, B. & Auwerx, J. Peroxisome proliferator-activated receptors, orphans with ligands and functions. *Curr Opin Lipidol* **8**, 159-166 (1997).
68. Berger, J. & Moller, D.E. The mechanisms of action of PPARs. *Annu Rev Med* **53**, 409-435 (2002).

69. Krey, G.*, et al.* Xenopus peroxisome proliferator activated receptors: genomic organization, response element recognition, heterodimer formation with retinoid X receptor and activation by fatty acids. *J Steroid Biochem Mol Biol* **47**, 65-73 (1993).
70. Issemann, I. & Green, S. Activation of a member of the steroid hormone receptor superfamily by peroxisome proliferators. *Nature* **347**, 645-650 (1990).
71. Lemberger, T.*, et al.* PPAR tissue distribution and interactions with other hormone-signaling pathways. *Ann N Y Acad Sci* **804**, 231-251 (1996).
72. Braissant, O., Foufelle, F., Scotto, C., Dauça, M. & Wahli, W. Differential expression of peroxisome proliferator-activated receptors (PPARs): tissue distribution of PPAR-alpha, -beta, and -gamma in the adult rat. *Endocrinology* **137**, 354-366 (1996).
73. Syversen, U.*, et al.* Different skeletal effects of the peroxisome proliferator activated receptor (PPAR)α agonist fenofibrate and the PPARγ agonist pioglitazone. *BMC Endocrine Disorders* **9**, 10 (2009).
74. Muoio, D.M.*, et al.* Fatty acid homeostasis and induction of lipid regulatory genes in skeletal muscles of peroxisome proliferator-activated receptor (PPAR) alpha knock-out mice. Evidence for compensatory regulation by PPAR delta. *J Biol Chem* **277**, 26089-26097 (2002).
75. Saltiel, A.R. & Olefsky, J.M. Thiazolidinediones in the treatment of insulin resistance and type II diabetes. *Diabetes* **45**, 1661-1669 (1996).
76. Willson, T.M., Brown, P.J., Sternbach, D.D. & Henke, B.R. The PPARs: From Orphan Receptors to Drug Discovery. *Journal of Medicinal Chemistry* **43**, 527-550 (2000).
77. Sertznig, P., Seifert, M., Tilgen, W. & Reichrath, J. Present concepts and future outlook: function of peroxisome proliferator-activated receptors (PPARs) for pathogenesis, progression, and therapy of cancer. *J Cell Physiol* **212**, 1-12 (2007).
78. Kersten, S., Desvergne, B. & Wahli, W. Roles of PPARs in health and disease. *Nature* **405**, 421-424 (2000).
79. Wang, Y.X.*, et al.* Peroxisome-proliferator-activated receptor delta activates fat metabolism to prevent obesity. *Cell* **113**, 159-170 (2003).
80. Chevillotte, E., Rieusset, J., Roques, M., Desage, M. & Vidal, H. The regulation of uncoupling protein-2 gene expression by omega-6 polyunsaturated fatty acids in human skeletal muscle cells involves multiple pathways, including the nuclear receptor peroxisome proliferator-activated receptor beta. *J Biol Chem* **276**, 10853-10860 (2001).
81. Mueller, E.*, et al.* Genetic analysis of adipogenesis through peroxisome proliferator-activated receptor gamma isoforms. *J Biol Chem* **277**, 41925-41930 (2002).
82. Staels, B.*, et al.* Mechanism of action of fibrates on lipid and lipoprotein metabolism. *Circulation* **98**, 2088-2093 (1998).
83. Kahn, S.E.*, et al.* Glycemic durability of rosiglitazone, metformin, or glyburide monotherapy. *N Engl J Med* **355**, 2427-2443 (2006).
84. Guan, Y. Peroxisome Proliferator-Activated Receptor Family and Its Relationship to Renal Complications of the Metabolic Syndrome. *Journal of the American Society of Nephrology* **15**, 2801 (2004).
85. Qu, B.*, et al.* Sirtuin1 promotes osteogenic differentiation through downregulation of peroxisome proliferator-activated receptor γ in MC3T3-E1 cells. *Biochem Biophys Res Commun* **478**, 439-445 (2016).
86. Kim, Y.-H.*, et al.* Fenofibrate induces PPARα and BMP2 expression to stimulate osteoblast differentiation. *Biochemical and Biophysical Research Communications* **520**, 459-465 (2019).
87. Scholtysek, C.*, et al.* PPARβ/δ governs Wnt signaling and bone turnover. *Nature Medicine* **19**, 608-613 (2013).
88. Still, K., Grabowski, P., Mackie, I., Perry, M. & Bishop, N. The peroxisome proliferator activator receptor alpha/delta agonists linoleic acid and bezafibrate upregulate osteoblast differentiation and induce periosteal bone formation in vivo. *Calcif Tissue Int* **83**, 285-292 (2008).

89. Mabilleau, G., Mieczkowska, A. & Edmonds, M.E. Thiazolidinediones induce osteocyte apoptosis and increase sclerostin expression. *Diabet Med* **27**, 925-932 (2010).
90. Carmona, M.C.*, et al.* Fenofibrate prevents Rosiglitazone-induced body weight gain in ob/ob mice. *Int J Obes (Lond)* **29**, 864-871 (2005).
91. Araki, M.*, et al.* The Peroxisome Proliferator-Activated Receptor α (PPARα) Agonist Pemafibrate Protects against Diet-Induced Obesity in Mice. *Int J Mol Sci* **19**(2018).
92. Harrington, W.W.*, et al.* The Effect of PPARalpha, PPARdelta, PPARgamma, and PPARpan Agonists on Body Weight, Body Mass, and Serum Lipid Profiles in Diet-Induced Obese AKR/J Mice. *PPAR Res* **2007**, 97125 (2007).
93. Garbacz, W.G., Huang, J.T., Higgins, L.G., Wahli, W. & Palmer, C.N. PPARα Is Required for PPARδ Action in Regulation of Body Weight and Hepatic Steatosis in Mice. *PPAR Res* **2015**, 927057 (2015).
94. Kim, J.C. The effect of exercise training combined with PPARγ agonist on skeletal muscle glucose uptake and insulin sensitivity in induced diabetic obese Zucker rats. *J Exerc Nutrition Biochem* **20**, 42-50 (2016).
95. Gregoire, F.M.*, et al.* MBX-102/JNJ39659100, a novel peroxisome proliferator-activated receptor-ligand with weak transactivation activity retains antidiabetic properties in the absence of weight gain and edema. *Mol Endocrinol* **23**, 975-988 (2009).
96. Zhang, J.*, et al.* The role of lipocalin 2 in the regulation of inflammation in adipocytes and macrophages. *Mol Endocrinol* **22**, 1416-1426 (2008).
97. Wang, D.*, et al.* Isolation and characterization of MC3T3-E1 preosteoblast subclones with distinct in vitro and in vivo differentiation/mineralization potential. *Journal of Bone and Mineral Research* **14**, 893-903 (1999).
98. Bonewald, L.F. The amazing osteocyte. *Journal of bone and mineral research* **26**, 229-238 (2011).
99. Jansson, J.O.*, et al.* Body weight homeostat that regulates fat mass independently of leptin in rats and mice. *Proc Natl Acad Sci U S A* **115**, 427-432 (2018).

Appendix

Appendix 1: Mouse Lipocalin-2/NGAL DuoSet ELISA protocol (R&D Systems)

Appendix 2: RNeasy Mini Kit protocol (p.25-28) (Qiagen)

Appendix 3: Individual biological replicates of Lipocalin 2 corrected to total protein concentration in MLO-Y4 cells, measured by ELISA.

Appendix 4: Individual biological replicates of Lipocalin 2 concentration in medium from MLO-Y4 culture, measured by ELISA.

Appendix 1: Mouse Lipocalin-2/NGAL DuoSet ELISA protocol (R&D Systems)

Reagent preparation (page 5):

Bring all reagents to room temperature before use. Allow all components to sit for a minimum of 15 minutes with gentle agitation after initial reconstitution. Working dilutions should be prepared and used immediately.

Streptavidin-HRP B: 2.0 mL of streptavidin conjugated to horseradish-peroxidase. Dilute to the working concentration specified on the vial label using Reagent Diluent.

Rat Anti-Mouse Lipocalin-2 Capture Antibody: Refer to the lot-specific C of A for amount supplied. Reconstitute each vial with 0.5 mL of PBS. Dilute in PBS without carrier protein to the working concentration indicated on the C of A.

Biotinylated Rat Anti-Mouse Lipocalin-2 Detection Antibody: Refer to the lot-specific C of A for amount supplied. Reconstitute each vial with 1.0 mL of Reagent Diluent. Dilute in Reagent Diluent to the working concentration indicated on the C of A.

Recombinant Mouse Lipocalin-2 Standard: Refer to the lot-specific C of A for amount supplied. Reconstitute each vial with 0.5 mL of Reagent Diluent. A seven point standard curve using 2-fold serial dilutions in Reagent Diluent is recommended. Prepare 1000 µL of high standard per plate assayed at the concentration indicated on the C of A.

General ELISA protocol (page 6):

Plate preparation

1. Dilute the Capture Antibody to the working concentration in PBS without carrier protein. Immediately coat a 96-well microplate with 100 µL per well of the diluted Capture Antibody. Seal the plate and incubate overnight at room temperature.
2. Aspirate each well and wash with Wash Buffer, repeating the process two times for a total of three washes. Wash by filling each well with Wash Buffer (400 µL) using a squirt bottle, manifold dispenser, or auto washer. Complete removal of liquid at each step is essential for good performance. After the last wash, remove any remaining Wash Buffer by aspirating or by inverting the plate and blotting it against clean paper towels.
3. Block plates by adding 300 µL of Reagent Diluent to each well. Incubate at room temperature for a minimum of 1 hour.
4. Repeat the aspiration/wash as in step 2. The plates are now ready for sample addition.

Assay procedure

1. Add 100 µL of sample or standards in Reagent Diluent, or an appropriate diluent, per well. Cover with an adhesive strip and incubate 2 hours at room temperature.

2. Repeat the aspiration/wash as in step 2 of Plate Preparation

3. Add 100 µL of the Detection Antibody, diluted in Reagent Diluent, to each well. Cover with a new adhesive strip and incubate 2 hours at room temperature.

4. Repeat the aspiration/wash as in step 2 of Plate Preparation.

5. Add 100 µL of the working dilution of Streptavidin-HRP B to each well. Cover the plate and incubate for 20 minutes at room temperature. Avoid placing the plate in direct light.

6. Repeat the aspiration/wash as in step 2.

7. Add 100 µL of Substrate Solution to each well. Incubate for 20 minutes at room temperature. Avoid placing the plate in direct light.

8. Add 50 µL of Stop Solution to each well. Gently tap the plate to ensure thorough mixing.

9. Determine the optical density of each well immediately, using a microplate reader set to 450 nm. If wavelength correction is available, set to 540 nm or 570 nm. If wavelength correction is not available, subtract readings at 540 nm or 570 nm from the readings at 450 nm. This subtraction will correct for optical imperfections in the plate. Readings made directly at 450 nm without correction may be higher and less accurate.7

Appendix 2: RNeasy Mini Kit protocol (p.25-28) (Qiagen)

Reagent preparation:

Add β-mercaptoethanol (β-ME) to RTL buffer before use (10 µl β-ME for 1ml RTL buffer).

Add ethanol (96 %) to RPE buffer before use (e4 x volume)

Procedure:

1. Harvest cells. Lyse cells directly in culture dish. For 6 well plate: completely aspirate cell-culture medium, wash twice with cold PBS (~2 ml for each well), and continue immediately with step 2 of the protocol. Incomplete removal of the cell-culture medium will inhibit lysis and dilute the lysate, affecting the conditions for binding of RNA to the RNeasy silica-gel membrane. Both effects may reduce RNA yield.

2. Disrupt cells by addition of Buffer RLT (350 µl RTL/well, NB with β-mercaptoethanol. Collect cell lysate with a rubber policeman.

3. Pipet lysate into a microcentrifuge tube. Vortex or pipet to mix and ensure that no cell clumps are visible before proceeding.

4. Homogenize the sample. Pass the lysate 5-10 times through a 20-gauge needle (0.9 mm diameter) fitted to an RNase-free syringe. Freeze homogenized lysate (-80°C) for later total RNA isolation.

All steps after this is performed at room temperature.

5. If frozen lysate, thaw samples on ice before proceeding. Add 1 volume (350 µl) of 70% ethanol to the homogenized lysate and mix well by pipetting. Do not centrifuge. Note: Visible precipitates may form after the addition of ethanol when preparing RNA from certain cell lines, but this will not affect the RNeasy procedure.

6. Apply up to 700 µl of the sample, including any precipitate that may have formed, to a labelled RNeasy mini column placed in a 2 ml collection tube (supplied). Close the tube gently, and centrifuge for 15 s at max speed. Discard the flow through. Reuse the collection tube in step 7.

7. Add 700 µl Buffer RW1 to the RNeasy column. Close the tube gently, and centrifuge for 15 s at maximum speed to wash the column. Discard the flow-through and collection tube.

8. Transfer the RNeasy column into a new 2 ml collection tube (supplied). Pipet 500 µl Buffer RPE (make sure ethanol is added to Buffer RPE before use) onto the RNeasy column. Close the tube gently, and centrifuge for 15 s at max speed to wash the column. Discard the flow-through. Reuse the collection tube in step 9.

9. Add another 500 µl Buffer RPE to the RNeasy column. Close the tube gently, and centrifuge for 2 min at max speed to dry the RNeasy silica-gel membrane. Continue directly with step 10.

It is important to dry the RNeasy silica-gel membrane since residual ethanol may interfere with downstream reactions. This centrifugation ensures that no ethanol is carried over during elution. Note: Following the centrifugation, remove the RNeasy mini column from the collection tube carefully so the column does not contact the flow-through as this will result in carryover of ethanol.

10. Place the RNeasy column in a new 2 ml collection tube (not supplied) and discard the old collection tube with the flow-through. Centrifuge in a microcentrifuge at full speed for 1 min.

11. To elute, transfer the RNeasy column to a new 1.5 ml collection tube (supplied). Pipet 20 µl RNase-free water directly onto the RNeasy silica-gel membrane. Close the tube gently, and centrifuge for 1 min at max speed to elute.

12. If the expected RNA yield is > 30 µg, repeat the elution step (step 9) as described with a second volume of RNase-free water. Elute into the same collection tube. Place RNA samples on ice and freeze at -80°C until further analyses.

Appendix 3: Individual biological replicates of Lipocalin 2 corrected to total protein concentration in MLO-Y4 cells, measured by ELISA.

Exposure time	Samples	Exp 1	Exp 2	Exp 3
24h	CTR 0.1%	1.128022614	2.535107736	0.919083623
	Feno 1µM	3.2001784	1.059969331	0.294840443
	CTR 1%	1.87860947	0.248240535	0.840488041
	Feno 10µM	2.395033991	0.932534718	0.92999264
72h	CTR 0.1%	4.885170728	5.423255472	3.755256144
	Feno 1µM	30.41239157	2.981830671	2.44317031
	CTR 1%	21.69108196	1.985674978	0.2299853
	Feno 10µM	8.902284562	1.060049528	1.351539681

Cells were incubated with control (DMSO 0.1% and 1%) and fenofibrate (1 and 10 µM) dissolved in DMSO for 24 and 72 hours. Three independent experiments are included, and data are presented as mean. Data are shown as percentage changes in relation to control.

Appendix 4: Individual biological replicates of lipocalin 2 concentration in medium from MLO-Y4 culture, measured by ELISA.

Exposure time	Samples	Exp 1	Exp 2	Exp 3
24h	CTR 0.1%	1606.05	4613.26	1343.705
	Feno 1µM	5884.29	1702.315	779.27
	CTR 1%	3229.195	1400.615	1566.43
	Feno 10µM	3678.005	1277.195	1223.63
72h	CTR 0.1%	18270.4	20241.9	61732
	Feno 1µM	100991.15	58324.8	54163.25
	CTR 1%	38208.65	7531.15	17812.525
	Feno 10µM	31376.925	14591.925	4555.175

Cells were incubated with control (DMSO 0.1% and 1%) and fenofibrate (1 and 10 µM) dissolved in DMSO for 24 and 72 hours. Three independent experiments are included, and data are presented as mean. Data are shown as percentage changes in relation to control.